

The torus instability

B. Kliem¹ and T. Török²

¹*Astrophysical Institute Potsdam, An der Sternwarte 16, 14482 Potsdam, Germany*

²*Mullard Space Science Laboratory, Holmbury St. Mary, Dorking, Surrey RH5 6NT, UK*

(Received 28 April 2006; accepted 23 May 2006)

The expansion instability of a toroidal current ring in low-beta magnetized plasma is investigated. Qualitative agreement is obtained with experiments on spheromak expansion and with essential properties of solar coronal mass ejections (CMEs), unifying the two apparently disparate classes of fast and slow CMEs.

We consider the expansion instability of a toroidal current ring with the goal to describe the rapid expansion of such rings or partial rings observed in laboratory and astrophysical plasmas [1, 2]. The equilibrium of this configuration was established by Shafranov and is realized in the tokamak fusion device [3]. It necessarily includes an external poloidal magnetic field \mathbf{B}_{ex} , since the Lorentz-self force, also referred to as the hoop force, as well as the net pressure gradient force of a bent current channel always point radially outward.

The stability of the Shafranov equilibrium has been considered by Bateman [4], who found that the ring is unstable against expansion if the external poloidal field decreases sufficiently rapidly in the direction of the major torus radius R . Since the hoop force decreases if the ring expands, a perturbation $dR > 0$ will be unstable if the opposing Lorentz force due to \mathbf{B}_{ex} decreases faster with increasing R than the hoop force. Bateman derived

$$n = -R d \ln B_{\text{ex}} / dR > 3/2 \quad (1)$$

as condition for the instability, which we will refer to as the torus instability (TI). If the field is purely poloidal, the TI can be regarded as a lateral kink instability distributed uniformly over the ring. If the equilibrium includes a toroidal field component inside the torus, as e.g. in the force-free case, the instability is driven in addition by the tendency of the toroidal component to straighten the field lines (opposite to its effect on the helical kink).

The TI is suppressed in fusion devices by employing external poloidal fields with sufficiently small decay indices n and by stabilizing image currents in the walls of the device. However, it may occur in astrophysical plasmas, where the external poloidal field is often strongly inhomogeneous [5], and in some plasma experiments [1, 6, 7]. In particular, the observations of erupting prominences on the Sun, which often evolve into the cores of coronal mass ejections (CMEs) causing major perturbations of the space weather [8], suggest the topology of a single expanding partial current ring, whose footpoints are anchored in the inertial visible solar surface. A threshold of $n > 2$ was estimated for this case [5]; otherwise the instability has apparently never been reconsidered. Research on CMEs was instead directed at the possibility of a catastrophe due to nonexistence of equilibrium in part

of parameter space [2, 9].

In the present Letter we derive a TI threshold that is somewhat more general than Eq. (1) and treat the evolution of the instability for the first time. We consider two cases: a freely expanding ring relevant in the laboratory and for CMEs, and an expanding ring with constant total current, which captures an important effect of the footpoint anchoring on an expanding partial ring and can be relevant in the initial stage of CMEs. We focus on the essence of the instability and its development by including only the hoop force (in the large aspect ratio approximation, $R \gg b$) and the stabilizing Lorentz force due to \mathbf{B}_{ex} . Gravity, pressure, external toroidal fields, and any variation in the direction of the minor radius b are neglected to permit a largely analytical description. The neglect of pressure effects is justified by the fact that the instability is primarily relevant for low-beta plasmas, in which the conversion of the stored magnetic energy is able to drive a large-scale expansion (their inclusion reduces the growth rate of the instability but does not alter its qualitative properties).

With these assumptions, the force balance is purely in the direction of the major radius and given by [3, 4]

$$\rho_m \frac{d^2 R}{dt^2} = \frac{I^2}{4\pi^2 b^2 R^2} (L + \mu_0 R/2) - \frac{I B_{\text{ex}}(R)}{\pi b^2}, \quad (2)$$

where ρ_m is the mass density of the ring and I is the total ring current. The inductance of the ring is given by $L = \mu_0 R (\ln(8R/b) - 2 + l_i/2)$. The internal inductance per unit length of the ring l_i is of order unity if the radial profile of the current density is not strongly peaked in the center of the torus; in particular for uniform current density, $l_i = 1/2$. The flux enclosed by the ring is $\Psi = \Psi_I + \Psi_{\text{ex}}$, with $\Psi_I = LI$. Ideal MHD requires $\Psi = \text{const}$ during a perturbation $R \rightarrow R + dR$. We now have to make an assumption how Ψ_{ex} evolves. Here we follow Bateman, who ignored changes in the external field due to the perturbation and evaluated the enclosed external flux using the prescribed external field $B_{\text{ex}}(R)$,

$$\Psi = \Psi_I + \Psi_{\text{ex}} = LI - 2\pi \int_0^R B_{\text{ex}}(r) r dr. \quad (3)$$

This consistency with the use of $B_{\text{ex}}(R)$ in the expression for the restoring force in Eq. (2) implies inconsistency regarding the conservation of the enclosed flux. If the latter

were to be treated consistently, one would have to require $\Psi_{\text{ex}}(R) = \text{const}$ instead. Numerical simulations of the instability, which will be reported elsewhere, support the instability criterion derived from Eq. (3). They also show that magnetic reconnection sets in at the rear side of the expanding ring as the instability develops and lets the ring effectively “slide” through the external poloidal field [10], so that Eq. (3) represents a reasonable approximation also for large expansions. With both assumptions for $\Psi_{\text{ex}}(R)$ it is easily seen that the total ring current, $I(R) \leq \Psi_{I0}/L(R)$, must decrease as a free torus expands, since the logarithmic term in L varies only weakly with R (subscripts 0 denote initial values here and henceforth).

We make the ansatz that $B_{\text{ex}}(R) = \hat{B}R^{-n}$ in the region of interest, $R \geq R_0$. (At $R \rightarrow 0$ a finite B_{ex} is assumed, whose particular value will drop out of the equations below. We also have to assume $n \neq 2$ in intermediate steps of the calculation but find that the final expressions [r.h.s. of Eq. (6) and following] match smoothly as $(n-2) \rightarrow \pm 0$.) Using Eq. (3) the ring current is expressed through the initial values,

$$I(R) = \frac{c_0 R_0 I_0}{cR} \left\{ 1 + \frac{c_0 + 1/2}{2c_0} \frac{1}{2-n} \left[\left(\frac{R}{R_0} \right)^{2-n} - 1 \right] \right\}, \quad n \neq 2, \quad (4)$$

where $c = L/(\mu_0 R)$. Inserting this in Eq. (2) and normalizing, $\rho = R/R_0$ and $\tau = t/T$, where

$$T = \left(\frac{c_0 + 1/2}{4} \frac{b_0^2}{B_{\text{eq}}^2 / \mu_0 \rho_{m0}} \right)^{1/2} = \frac{(c_0 + 1/2)^{1/2}}{2} \frac{b_0}{V_{\text{Ai}}} \quad (5)$$

is essentially the “hybrid” Alfvén time of the minor radius (based on the external equilibrium field $B_{\text{eq}} = B_{\text{ex}}(R_0)$ and the initial density in the torus), we obtain the equation describing the evolution of the major radius

$$\frac{d^2 \rho}{d\tau^2} = \frac{c_0^2}{(c_0 + 1/2)c} \rho^{-2} \left[1 + \frac{c_0 + 1/2}{c_0} \frac{\rho^{2-n} - 1}{2(2-n)} \right] \left\{ \frac{c + 1/2}{c} \left[1 + \frac{c_0 + 1/2}{c_0} \frac{\rho^{2-n} - 1}{2(2-n)} \right] - \frac{c_0 + 1/2}{c_0} \rho^{2-n} \right\}, \quad n \neq 2. \quad (6)$$

We now assume $c(R) = \text{const}$, which is exact if the expansion is self-similar and can otherwise be expected to introduce relatively little error because c depends only logarithmically on $R/b(R)$. An approximately self-similar evolution of a freely expanding ring has been found in a laboratory experiment [1], and also the observations of CMEs indicate some degree of self-similarity [11]. With $c(R) = c_0$, the condition for instability, $d(d^2 \rho / d\tau^2) / d\rho|_{\rho=1} > 0$, becomes

$$n > n_{\text{cr}} = 3/2 - 1/(4c_0). \quad (7)$$

Bateman’s condition is recovered as $c_0 \rightarrow \infty$, which may be regarded as the “very large aspect ratio limit.” If $\Psi_{\text{ex}}(R) = \Psi_{\text{ex}0}$ is assumed in Eq. (3), then the expansion is described by $d^2 \rho / d\tau^2 = (c_0/c)^2 (c + 1/2)/(c_0 + 1/2) \rho^{-2} [1 - \rho^{2-n} (c/c_0)(c_0 + 1/2)/(c + 1/2)]$ instead of Eq. (6), and (again with $c(R) = c_0$) the threshold rises to $n > 2$. We note that this assumption (with $\Psi_{\text{ex}0} = 0$) and this threshold correspond to the case of a gravitationally balanced current ring around a star or massive object, which should, therefore, be marginally stable.

Eq. (6) can be integrated twice only for small displacements, $0 < \epsilon = \rho - 1 \ll 1$, showing that the expansion starts nearly exponentially,

$$\epsilon(\tau) = \frac{v_0 T / R_0}{(n - n_{\text{cr}})^{1/2}} \sinh \left((n - n_{\text{cr}})^{1/2} \tau \right), \quad \epsilon \ll 1, \quad (8)$$

with the growth rate $\gamma = (n - n_{\text{cr}})^{1/2}$. Here v_0 is the initial velocity of the expansion resulting from a perturbation. Integrating Eq. (6) once shows that for $n > 3/2$ a constant asymptotic velocity is reached

$$v_\infty = \left[\left(\frac{v_0 T}{R_0} \right)^2 + \frac{2(2n - 3 + \frac{1}{2c_0})(n - 1 + \frac{1}{4c_0})}{(2n - 3)(n - 1)} \right]^{1/2} \approx [(v_0 T / R_0)^2 + 2]^{1/2}, \quad n > 3/2. \quad (9)$$

For $n_{\text{cr}} < n < 3/2$ the acceleration does not decrease sufficiently rapidly as $\rho \rightarrow \infty$ so that the asymptotic velocity diverges. This discrepancy with the behavior at $n > 3/2$ results from the simplifications made; it would disappear if the restoring forces due to flux and pressure pileup in front of the expanding ring, which dominate at large ρ , would be included. The asymptotic gain of kinetic energy is $\Delta W = M \int_{R_0}^{\infty} (d^2 R / dt^2) dR \approx M (R_0 / T)^2$, $n > 3/2$, where $M = 2\pi^2 b_0^2 R_0 \rho_{m0}$ is the mass of the torus.

For large aspect ratio, the characteristic velocity in these expressions is much larger than the hybrid Alfvén velocity of the initial configuration, $R_0 / T \approx (R_0 / b_0) V_{\text{Ai}} \gg V_{\text{Ai}}$ (with $l_i \sim 1/2$ we have $(c_0 + 1/2)^{1/2} / 2 \approx 1$). Therefore, $v_0 T / R_0 \ll 1$ even in the case that the initial perturbation v_0 approaches V_{Ai} , as may happen if it is due to a kink instability [10, 12]. The dimensional asymptotic expansion velocity, $\approx 2^{1/2} (R_0 / b_0) V_{\text{Ai}}$ for $n > 3/2$, scales as the Alfvén velocity of the initial configuration.

Figure 1 shows the acceleration profile, $a = d^2 \rho / d\tau^2$, and the numerical solution of Eq. (6) with $c(R) = c_0$, along with the analytical approximations Eqs. (8) and (9), for particular values of $v_0 T / R_0$ and R_0 / b_0 and for the practically relevant range of n . The acceleration rises quickly to a maximum, which increases strongly with $n > n_{\text{cr}}$ and is reached within $\rho \lesssim 2$ for all n shown. It then decreases quickly with increasing ρ for $n \gtrsim 2$ but decreases only slowly for n close to n_{cr} . The resulting expansion, $\rho(\tau) - 1$, has an approximately exponential-to-linear characteristic for $n \gtrsim 2$, but is much closer

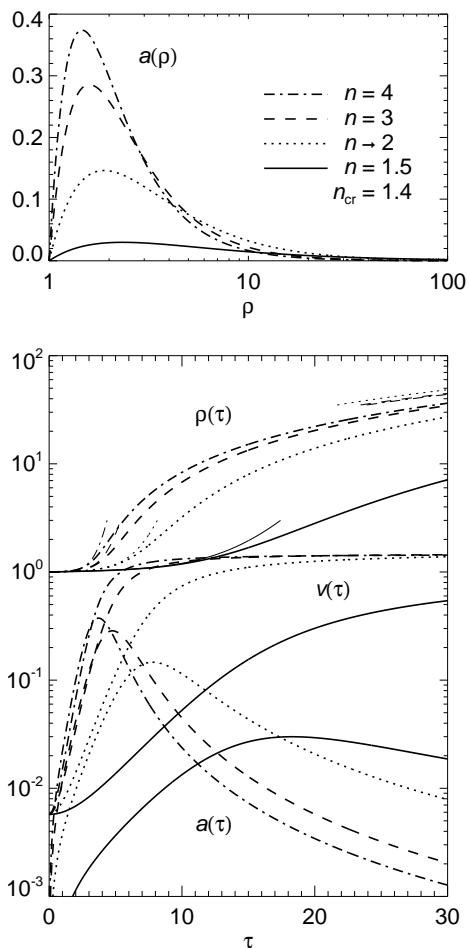


FIG. 1: Radial acceleration profiles and solutions of Eq. (6) for the freely expanding torus with $c(R) = \text{const}$ and $R_0/b_0 = 10$, $v_0 T/R_0 = 0.005$, $l_i = 1/2$. The approximate solutions, Eqs. (8, 9), are included as thin lines.

to a constant-acceleration curve over a considerable radial range for n close to n_{cr} . A qualitatively similar n dependence of the acceleration profile is obtained if $\Psi_{\text{ex}}(R) = \Psi_{\text{ex}0}$ is assumed in Eq. (3).

This n dependence of the expansion fits perfectly to the typical characteristics of CME rise profiles. Fast CMEs reach a speed of $\sim 10^3 \text{ km s}^{-1}$, comparable to the Alfvén velocity in the inner corona, often within a height range of $h \lesssim R_\odot/3$ above the photosphere and show no significant acceleration further out. These events originate from active regions which possess a rapid decay of the field concentration at heights comparable to the sunspot distance D ($D \sim R_\odot/10$ in bigger active regions); for essentially bipolar active regions, $n > 3/2$ for $h > D/2$, quickly approaching $n \approx 3$ at $h \gtrsim D$. On the other hand, slow CMEs propagate with roughly constant, small acceleration throughout the currently observable height range ($h \lesssim 30 R_\odot$), reaching the gravitational escape speed of a few 10^2 km s^{-1} typically only at heights of several R_\odot . These events originate from erupting prominences

far from active regions, where the large-scale height dependence of the field, approximately $B \propto h^{-3/2}$ [13], dominates already low in the corona. Interestingly, the fastest CMEs, and the strongest flares, originate in so-called δ -spot regions, which are quadrupolar, with one pair of opposite polarity being closely packed within a single sunspot, so that a particularly steep field decrease ($n > 3$) occurs low in the corona within very strong fields, which imply high Alfvén velocities of up to several 10^3 km s^{-1} . Thus, the torus instability not only provides a uniform description of the apparently disparate classes of fast and slow CMEs [14] but explains naturally also the preferred occurrence of the most powerful solar eruptions in δ -spot regions [15].

The magnetic field in erupting prominences and CME cores can be modeled as a section of a torus, whose remaining part is submerged and frozen in the dense, high-beta photospheric and subphotospheric plasma. Such line-tying is generally regarded to have a stabilizing influence; for example, in case of the helical kink instability it raises the threshold twist from 2π to 2.49π [16]. It has an even stronger effect on the TI. If a current-carrying loop emerges or is formed in the low corona, the line-tying is expected to suppress the instability completely until the loop is at least semicircular, since the major radius of a rising loop must *decrease* before that stage [17]. Beyond that point, however, the line-tying introduces a strong support of the expansion because it enforces the current through the footpoints of the partial ring to be constant. It is not clear at present how much of this current can enter the coronal part of the ring, where, due to the low resistivity, reconnection cannot easily occur so that the number of field line turns within the ring and hence IR tend to be constant. While a complete account of the line-tying requires a more sophisticated treatment, we can describe its amplifying effect on the expansion by replacing Eq. (4) with $I(R) = I_0$, obtaining the limiting case of maximum outward acceleration, given by

$$\frac{d^2\rho}{d\tau^2} = \frac{1}{2(c_0 + 1/2)} + \frac{(2n - 3)c_0 + 1/2}{2(n - 2)(c_0 + 1/2)}\rho^{-1} - \frac{2n - 3}{2(n - 2)}\rho^{1-n}, \quad n \neq 2. \quad (10)$$

The critical decay index of the external poloidal field for instability,

$$n_{\text{cr}} = 3/2 - 1/(2c_0 + 1), \quad (11)$$

is only slightly smaller than the critical index for the freely expanding ring. The initial evolution is again given by Eq. (8). The strong amplifying effect becomes apparent in the further evolution. This shows an enlarged radial range of acceleration, in better agreement with CME observations, and a higher peak (Fig. 2). The asymptotic acceleration does not vanish, however. Since $a(\rho \rightarrow \infty)$ is small only for $\ln(8R_0/b_0) \gg 1$ or for $l_{i0} \gg 1$, which

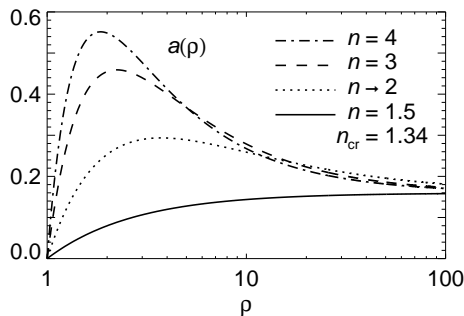


FIG. 2: Radial acceleration profiles of the torus instability with fixed ring current (Eq. 10) and parameters as in Fig. 1.

both do not have observational support, it is obvious that Eq. (10) cannot hold throughout the expansion.

Another consequence of constant ring current is the decrease of the aspect ratio in the course of the instability. Requiring $\Psi(R) = \Psi_0$ (Eq. 3) with $I(R) = I_0$, we find

$$\frac{b(R)}{R} = \frac{8}{\exp \left\{ c_0 \rho^{-1} + \frac{c_0 + 1/2}{2(n-2)} \rho^{-1} (1 - \rho^{2-n}) + 2 - \frac{L_i}{2} \right\}}, \quad n \neq 2, \quad (12)$$

(Fig. 3). Such overexpansion of the minor radius is a characteristic of many CMEs, observed as a cavity in the outer part of the rising flux, which gives rise to the so-called three-part structure of CMEs [8]. The overexpansion is so rapid that $b \rightarrow R$ for $\rho = R/R_0 \sim 10^1 - 10^2$. At this point our simplified description breaks down. We can expect that magnetic reconnection with the surrounding field or between the loop legs is then triggered. This implies that $I(R) = \text{const}$ no longer holds and that the acceleration falls off as the reconnection proceeds. Comparing the acceleration profiles in Figs. 1 and 2, it is clear that the association of fast and slow CMEs with, respectively, high and only slightly supercritical decay index n holds for line-tied current rings as well.

Let us finally consider the expansion of a spheromak-like torus in a nearly field-free vacuum chamber [1], which proceeded in the observed range, $\rho \lesssim 2$, with roughly constant velocity. We note that Taylor relaxation in the torus transformed toroidal into poloidal flux in the course of the expansion, influencing the TI in as yet unknown ways, and that the scatter in the data (Fig. 19 in [1]) permits a fit with slightly increasing velocity as well. With $\mathbf{B}_{\text{ex}} = 0$ and $\Psi(R) = L_0 I_0$ we obtain $d^2 \rho / d\tau^2 = (c+1/2)c^{-2}\rho^{-2}$ in place of Eq. (6), where time is now normalized to $T' = (\pi/c_0)(b_0/\tilde{V}_{\text{Ai}})$ and \tilde{V}_{Ai} is defined using the field in the center of the ring (\tilde{B}) and ρ_{m0} . This acceleration decreases so rapidly that, soon after onset, the expansion velocity is expected to increase only slowly with ρ , consistent with the observation. The asymptotic velocity, $((c+1/2)/c^2)^{1/2} R_0/T' \sim 5-16 \text{ kms}^{-1}$, obtained using the observed $R/b \approx 2$, $\tilde{B} \sim 300 \text{ G}$ as a representative value of the measured range (Figs. 11, 12b,c in

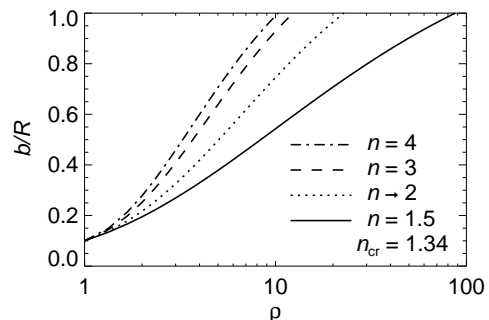


FIG. 3: Development of the inverse aspect ratio for the torus instability with fixed ring current (Eq. 12) for $R_0/b_0 = 10$.

[1]), and estimated densities $N \sim 10^{15} - 10^{16} \text{ cm}^{-3}$ (Bellan, personal communication), is in acceptable agreement with the observed expansion velocity of $\approx 5 \text{ km s}^{-1}$.

We conclude that the TI is a possible mechanism for CMEs (in addition to a catastrophe [2, 9] and to the helical kink instability [10]), that the TI governs their medium-scale ($\rho \lesssim 10^2$) expansion, providing a unified description of fast and slow CMEs and a possible explanation for their three-part structure, and that the TI occurred in experiments on spheromak expansion.

We gratefully acknowledge constructive comments by T. G. Forbes, P. Démoulin, and V. S. Titov. This work was supported by DFG and PPARC.

-
- [1] J. Yee and P. M. Bellan, *Phys. Plasmas* **7**, 3625 (2000).
 - [2] T. G. Forbes, *J. Geophys. Res.* **105**, 23153 (2000).
 - [3] V. D. Shafranov, *Rev. Plasma Phys.* **2**, 103 (1966).
 - [4] B. Bateman, *MHD Instabilities* (MIT, Cambridge, 1978).
 - [5] V. S. Titov and P. Démoulin, *Astron. Astrophys.* **351**, 707 (1999).
 - [6] J. F. Hansen and P. M. Bellan, *Astrophys. J.* **563**, L183 (2001).
 - [7] S. C. Hsu and P. M. Bellan, *Phys. Rev. Lett.* **90**, 215002 (2003).
 - [8] N. Crooker et al., eds., *Coronal Mass Ejections*, Geophysical Monogr. 99 (AGU, Washington, 1997).
 - [9] E. R. Priest and T. G. Forbes, *Astron. Astrophys. Rev.* **10**, 313 (2002).
 - [10] T. Török and B. Kliem, *Astrophys. J.* **630**, L97 (2005).
 - [11] V. Bothmer and R. Schwenn, *Space Sci. Rev.* **70**, 215 (1994).
 - [12] T. Török, B. Kliem, and V. S. Titov, *Astron. Astrophys.* **413**, L27 (2004).
 - [13] B. Vršnak, J. Magdalenic, H. Aurass, and G. Mann, *Astron. Astrophys.* **396**, 673 (2002).
 - [14] R. M. MacQueen and R. R. Fisher, *Solar Phys.* **89**, 89 (1983).
 - [15] I. Sammis, F. Tang, and H. Zirin, *Astrophys. J.* **540**, 583 (2000).
 - [16] A. W. Hood and E. R. Priest, *Geophys. Astrophys. Fluid Dyn.* **17**, 297 (1981).
 - [17] J. Chen and J. Krall, *J. Geophys. Res.* **108**, 1410 (2003).